

Analysis of Seismic Activity near Theodore Roosevelt Dam, Arizona, during the Occupation of the EarthScope/USArray Transportable Array

by **Jeffrey S. Lockridge, Matthew J. Fouch, J Ramón Arrowsmith, and Lepolt Linkimer**

Online Material: Plot of viable focal mechanisms and table of regional seismic velocity model.

INTRODUCTION

Rate and distribution of seismic activity are important indicators of the overall state of tectonic stress within a region. In regions characterized by low levels of seismicity, active fault surfaces are rarely visible at the surface, and the analysis of small-magnitude earthquakes at depth may be the most effective way to identify seismic hazard and risk from ambient tectonic activity. Further, studies of local and regional seismicity are also a direct way to examine geophysical and tectonic boundaries, although determining long-term seismicity levels requires good knowledge of the earthquake cycle. A major challenge in monitoring regions with low seismicity levels, therefore, is that long-term recording and/or deployment of sensitive instrumentation is required to provide adequate data.

Seismicity patterns are of particular concern near large population centers and key infrastructure, such as power plants and dams. For instance, the Phoenix metropolitan area in south-central Arizona receives its water through a network of canals fed by multiple man-made reservoirs located throughout the state. Analysis of seismicity patterns in the vicinity of these reservoirs and their associated dam structures is important because (1) the occurrence of an unexpectedly large earthquake may result in the failure of the dam structure resulting in adverse consequences to nearby human populations and the environment, and (2) the reservoir itself may induce seismicity and increase earthquake activity above previously recorded background levels (Simpson *et al.*, 1986; Talwani, 1997; Gupta, 2002).

The state of Arizona is a type example of a region where, until recently, little was known about regional-scale seismicity. The lack of historical earthquake monitoring across the region has precluded comprehensive seismicity studies, leading to the misperception that most of the state is seismically inactive relative to neighboring regions of the tectonically active

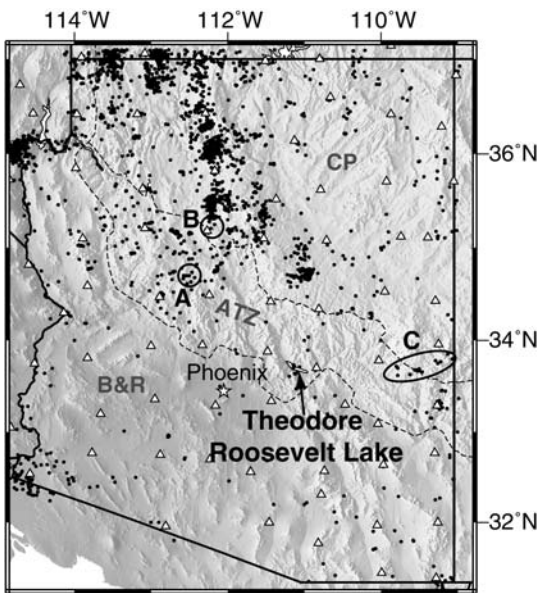
western United States. However, in a recent study, Lockridge *et al.* (2012) utilized data from the EarthScope USArray Transportable Array (TA) to develop the first spatially comprehensive catalog of seismicity for the state of Arizona that is complete to local magnitude (M_L) 1.2, providing a new starting point for improved tectonic analyses of the region.

In this study, we focus on a unique event cluster discovered by Lockridge *et al.* (2012), centered approximately 7 km northeast of Theodore Roosevelt Dam (Roosevelt Dam) and in central Arizona. We combine an evaluation of current and historical earthquake catalogs with a detailed analysis of TA data to build an event catalog containing all documented earthquakes in the area surrounding the Theodore Roosevelt Lake reservoir (Roosevelt Lake). We compute source mechanisms for the largest two events in the cluster, and use these to explore the current state of local crustal stress. Further, we evaluate the potential impact of reservoir loading and unloading on local seismicity by investigating temporal patterns of this cluster and its relationship to historical water levels.

REGIONAL GEOLOGIC SETTING

The state of Arizona comprises three distinct physiographic provinces: the Colorado Plateau (CP), Arizona Transition Zone (ATZ), and the southern Basin and Range (B&R; Fig. 1). A range of datasets, including crustal structure and thickness, stress orientations, volcanism, seismicity, heat flow, and gravity, suggest that the ATZ represents a tectonic transition between the thick and relatively stable crust of the CP and the thin and highly-extended crust of the southern B&R (Brumbaugh, 1987; Hendricks and Plescia, 1991; Thompson and Zoback, 1979; Frassetto *et al.*, 2006; Bashir *et al.*, 2011; Gilbert, 2012). However, these transitions do not strictly occur along the physiographic boundaries, and the tectonic evolution of the region remains enigmatic (e.g., Menges and Pearthree, 1989).

The topographic relief from the uplifted CP in northern Arizona to the thinned crust in the southern B&R province in southern Arizona was created by northeast–southwest crustal



▲ **Figure 1.** Physiographic and seismotectonic setting of Roosevelt Lake. Black dots represent historical earthquakes within Arizona from 1830 to May 2011 (Lockridge *et al.*, 2012). USArray TA stations (triangles) recorded the data used in this study. Boundaries between physiographic provinces (CP-Colorado Plateau; ATZ-Arizona Transition Zone; B&R-Basin and Range) are denoted as dashed lines (from Peirce, 1984). Circled areas highlight ATZ seismicity associated with (A) the 4 February 1976 m_b 4.9 Chino Valley earthquake (Eberhart-Phillips *et al.*, 1981), (B) the 4 November 1971 M_L 3.7 earthquake near Williams, Arizona (Brumbaugh, 1980), and (C) the swarm of 20 M_L 3.2–4.2 earthquakes in eastern Arizona (Eagar and Fouch, 2007).

extension that occurred during development of the B&R. The northwest–southeast least principal stress direction during B&R extension resulted in the formation of northwest trending mountain fault blocks (Zoback *et al.*, 1981) separated by large sediment-filled basins throughout the southern and central portions of the state. Dates for the extension of the B&R province range vary from 25–6 Ma (McQuarrie and Wernicke, 2005) to 15–5 Ma (Menges and Pearthree, 1989); however, studies agree that B&R tectonism has ceased in southern and central Arizona. Furthermore, seismotectonic investigations conducted on a statewide scale for Arizona (Menges and Pearthree, 1983; Pearthree *et al.*, 1983), on a regional scale for central Arizona (Pearthree and Scarborough, 1984), and at a local scale for Roosevelt Dam (Anderson *et al.*, 1987) agree that while known Quaternary faults within the ATZ are few, they generally trend in the northwest–southeast direction and are consistent with the reactivation of faults that originated during B&R extension.

Historical earthquake catalogs imply that the ATZ experiences low levels of seismic activity relative to regions in the northern portion of Arizona (e.g., Lockridge *et al.*, 2012). However, a few significant earthquakes have provided interesting hints of the deeper tectonic structure of the area. Analysis of the 4 February 1976 body wave magnitude (m_b) 4.9 Chino

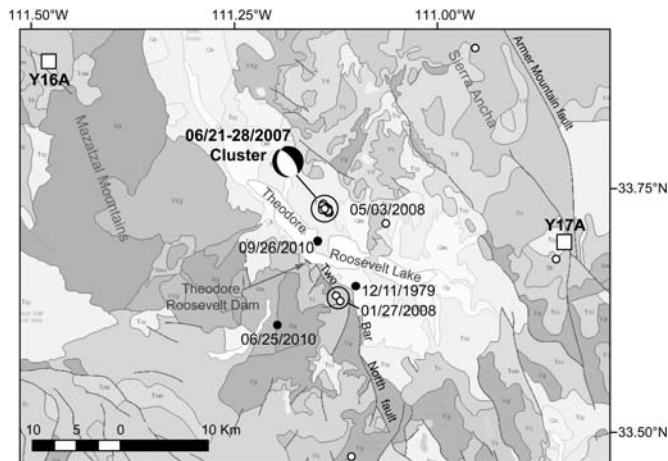
Valley earthquake identified a northwest trending normal fault plane with a 40° dip to the southwest as well as microseismicity in the area at a rate of 0.3 events per day (Eberhart-Phillips *et al.*, 1981). Nearly all focal mechanisms for earthquakes within the southernmost CP indicate northwest-trending normal faulting (Kreemer *et al.*, 2010 and references therein). The lone exception to this trend is the 4 November 1971 M_L 3.7 earthquake near Williams, Arizona, where Brumbaugh (1980) determined a focal mechanism consistent with northwest-trending high angle reverse faulting within a recently active volcanic field. An earthquake swarm containing at least twenty small (M_L 3.2–4.2) earthquakes was also identified in eastern Arizona within the southern CP (Eagar and Fouch, 2007), indicating that the region may be capable of releasing significant stress via repeated slip along previously unidentified subsurface faults.

Recent seismic activity within the ATZ has also been significant. Following the removal of the USArray TA from the region, and therefore not included in this study, we note that a number of swarms and moderate (M_L 3.5 and greater) earthquakes occurred within the ATZ. These include 13 earthquakes of duration magnitude (M_d) 2.0–2.7 from 21 to 26 June 2011 associated with the Lake Mary fault system southeast of Flagstaff, an M_L 3.7 earthquake located north of the town of Jerome on 18 March 2011, an M_L 3.5 earthquake located west of Sedona on 23 January 2011, an M_L 3.6 earthquake with ~17 aftershocks occurring near the Arizona-New Mexico border on 24 May 2010, and an M_L 3.6 earthquake located near Roosevelt Lake on 25 June 2010 (see Data and Resources section).

Here we focus in detail on seismicity near the area of Roosevelt Dam, located approximately 130 km northeast of Phoenix within the ATZ (Fig. 1). Roosevelt Dam was completed in 1911 within a narrow gorge just downstream from the confluence of Tonto Creek and the Salt River. Roosevelt Lake fills a large portion of the Tonto Basin, extending ~17 km upstream along the original Salt River bed and ~15 km along the original Tonto Creek bed. Tonto Basin is a northwest–southeast trending graben bounded by the horst blocks of the Mazatzal Mountains to the west and the Sierra Ancha to the east (Fig. 2). The lithology of Tonto Basin consists of Precambrian metamorphic, granitic, and sedimentary rocks and Paleozoic sedimentary rocks overlain by approximately 300 m of Tertiary sediments, with Quaternary gravel-capped pediments, alluvial fans, and stream terraces (Anderson *et al.*, 1987). Basin-bounding faults are poorly exposed in the area, but are identified as the Two Bar North fault to the southwest and the Armer Mountain fault to the northeast (Fig. 2). These faults both strike to the northwest, but recent studies have considered them to be inactive since they do not displace Quaternary basin-fill in the area (Pearthree and Scarborough, 1984; Anderson *et al.*, 1987).

METHODS

The USArray TA recorded broadband seismic data in the state of Arizona from April 2006 to March 2009. For a preliminary



▲ **Figure 2.** Total seismicity recorded in the area of Roosevelt Lake, including earthquakes recorded during the deployment of the EarthScope USArray TA (white circles) and events found in historical event catalogs (black dots; see [Data and Resources](#) section). Groups of spatially clustered events are circled. Displayed focal mechanism is a summary focal mechanism solution for the two largest (M_L 3.1 and 2.7) events in the June 2007 cluster. The two nearest TA stations used in this study are displayed as white squares. Background is a grayscale digital geologic map of Arizona (see [Data and Resources](#) section), where bedrock is displayed as darker grays, Tertiary and Quaternary sediments are light grays, and mapped inactive faults are solid black lines.

analysis of the spatial and temporal distributions of seismic activity within Arizona during this time period, we used USArray's Array Network Facility (ANF) monthly event catalog (see [Data and Resources](#) section) to generate a Google Earth file of events recorded by the TA. The ANF catalog includes events identified in other regional catalogs, as well as additional events located by an ANF automatic detection algorithm and confirmed by ANF analysts (see [Data and Resources](#) section). Using Google Earth to explore events from the ANF catalog, we identified 16 areas of seismicity within Arizona that exhibit event clusters with clear spatial and temporal correlations. We noted a spatial cluster of eight events adjacent to Roosevelt Lake that occurred during a five-day period from 21 June to 26 June 2007. The ANF located these events an average of approximately 6.5 km northeast of Roosevelt Dam, with hypocentral depths ranging from 8 to 17 km, and unknown magnitudes. Due to the proximity of the cluster to Roosevelt Dam and the potential human impact of seismicity in this area, we elected to further analyze the Roosevelt Lake cluster using data from the TA.

To generate a catalog containing all events contained within this cluster, we first reviewed waveform data from the eight TA stations nearest to the Roosevelt Lake cluster using the Antelope Environmental Data Collection Software (Antelope; see [Data and Resources](#) section). We visually scanned continuous data from these stations recorded between 21 June and 28 June 2007 to identify P and S wave arrivals. We used a

Butterworth bandpass filter with corner frequencies of 1 and 5 Hz to search for arrivals, and either a 0.3 Hz high-pass acausal filter or no bandpass filter to pick phase arrivals. To locate earthquake hypocenters, we used Antelope's *dbgenloc* software (Pavlis *et al.*, 2004) and a 1D seismic velocity model for the ATZ (see Table S1, available as an electronic supplement to this paper) from Sinno *et al.* (1981). Hypocentral error estimates using this methodology are addressed by Lockridge *et al.* (2012), who informally estimated lateral errors of ~ 1 –2 km and depth errors of ~ 5 km. Here we note that significant variations in 3-D crustal structure are likely to exist in this region, especially to the southwest where several stations used for this study are located within the B&R province and not the ATZ. We used Antelope's *orbevproc* program to calculate M_L for each event. This code follows the basic methodology first described by Richter (1935), whereby the largest 3-component peak amplitude is used and an empirical scaling factor based on assumed attenuation at the event's epicentral distance is applied. We note that at the time of data processing for this study, the ANF database did not include magnitudes for most small events, but now does report event magnitudes for most events in the ANF catalog.

To search for additional earthquakes within the Roosevelt Lake area during the TA deployment, we employed a similar event automatic detection scheme to that used by the ANF to process global seismicity using TA data (see Lockridge *et al.*, 2012). We applied a short-term average/long-term average (STA/LTA) amplitude detection algorithm (*dbdetect*) to the vertical channels of the eight stations nearest to the cluster. We used an STA window of 1.5 s, an LTA window of 10 s, and a Butterworth bandpass filter with corner frequencies of 0.5 and 5 Hz to detect any instances where the amplitude signal to noise (S/N) threshold was greater than 3.0. We then defined a travel time grid space (*ttgrid*) centered at the area of seismicity (33.74° N, 111.13° W), which spans 1° by 1° with 151 grid nodes on each axis, and depth layers spaced 2 km between 0 and 20 km, and spaced 5 km between 20 and 50 km. We utilized the event association program (*dbgrassoc*) to identify potential events where (1) P waves were detected on four or more stations within a 15-s time window, and (2) initial hypocenter locations were produced within the established travel-time grid. This process usually results in the detection of many spurious events when run at such a low S/N threshold so, following the automatic procedure, we manually inspected each potential event using the methods described by Lockridge *et al.* (2012) to identify mine blasts or other non-tectonic sources. In general, we identified mine blasts by emergent P and S arrivals, significant low frequency signal, and initial hypocenter locations in the direct area of mining-related surficial scarring observed in satellite imagery on Google Earth.

To test the sensitivity of our automatic detection algorithm, we compared the results from the automatic detection scheme with the events we picked manually during the period of peak seismicity from 21 June 2007 to 28 June 2007. Our automatic detection algorithm successfully identified 10 out of 10 events with $M_L > 1.0$, as well as two previously unidentified

events with $M_L < 1.0$ that occurred on 27 January 2008. However, our detection algorithm did not identify any of the 10 events with $M_L < 1.0$ that we picked manually during the period of peak seismicity, and it also did not detect an $M_L 1.0$ earthquake on 3 May 2008 with an epicenter approximately 10 km northeast of the dam that we located as part of a separate study on Arizona seismicity (Lockridge *et al.*, 2012). We attempted to improve our event detection threshold by lowering the S/N minimum and altering STA/LTA triggering windows in our automatic detection scheme, but were unable to detect smaller magnitude events without greatly increasing the number of spurious event detections. Based on these tests, we conclude that our detection algorithm is calibrated to successfully detect all events $M_L > \sim 1.0$ for this region at TA station spacing.

RESULTS

After a manual review of waveform data during the period of peak seismicity, we detected 62 events at one or more station, 20 of which were large enough to locate using four or more phase arrivals. By using the automatic detection algorithm described above, we detected two additional events on 27 January 2008. Many of these events exhibited similar waveform characteristics, which we discuss in more detail below.

The location of earthquake hypocenters within a spatially and temporally clustered set of events can be improved with use of a multichannel cross correlation or matched filter scheme. Unfortunately, these approaches are not likely to yield robust results for many of the events in this study due to their low S/N ratio. Furthermore, studies on other intraplate earthquake clusters (Ma and Eaton, 2009; Ma *et al.*, 2008; Uski *et al.*, 2006) have combined the regional phase modeling approach with double-difference methods (Ma and Eaton, 2011); however, these methods are utilized in regions with poor station coverage and we consider them unlikely to improve the hypocentral locations over the methods used in this study. To test the hypothesis that the Roosevelt Lake cluster was a series of repeating events occurring along the same fault, we visually examined the waveforms of each event in an effort to determine waveform similarities. Through this analysis, we identified three separate families of events. Of the 22 largest events, we identified 16 events in Family 1, four events in Family 2, and two (the two 27 January 2008 events) in Family 3 (Table 1; Fig. 3). The locations of events in Families 1 and 2 appear to be associated with slip along an unnamed lineament on the north side of the reservoir, while Family 3 events appear to be associated with the Two Bar North fault on the south side of the reservoir (Fig. 2). We were unable to evaluate temporal trends in hypocenter location and depth for events in the Roosevelt Lake cluster because all events within Families 1 and 2 are located within 1.5 km of one another, well within our estimated hypocentral error range.

Given the small number of earthquakes in the Roosevelt Lake cluster and the short time interval of the TA deployment, we determined that calculating b -values for the cluster would

not be useful or accurate. We note, however, that Lockridge *et al.* (2012) found a b -value of 0.91 in their study of Arizona-wide seismicity during the occupation of the TA. Therefore, to identify temporal trends in magnitude for the Roosevelt Lake cluster, we reviewed the chronological event list (Table 1) and found that the two largest events ($M_L 2.7$ and 3.1; waveform Family 1) are each immediately followed within the next 15 min by a series of 3–4 smaller aftershocks. We also observed that event frequency decreases with time following the two largest events, consistent with typical mainshock–aftershock sequences. Additionally, three out of four Family 2 events occur within a time window that spans from 2 min before to 15 min following the largest ($M_L 3.1$) event in the sequence (see Table 1). We speculate that the significantly different waveforms and therefore different focal mechanisms of the Family 2 events may represent post-event adjustments on the fault, which are accommodating strain changes caused by the larger events.

We also calculated first-motion focal mechanisms for the 2 largest events in the cluster ($M_L 2.7$ and 3.1) using the program FOCMEC (Snoke *et al.*, 1984) included in the version 8.3 of the SEISAN software package (Havskov and Ottemöller, 1999). This approach uses P -wave polarity as input and take-off angles that are calculated using a layered medium, and performs a grid search of the focal sphere to determine how many polarities fit each possible focal mechanism solution. Only a few clear SH polarities could be measured for these events, and the overall family of viable solutions was consistent enough that the inclusion of SH polarities would not have led to significantly improved focal mechanism solutions. We determined 11 P -wave polarities for the $M_L 3.1$ event and nine P -wave polarities for the $M_L 2.7$ event. We then performed a grid search over 5-degree increments in azimuth and take-off angle to find zero polarity errors. Based on this methodology, we found suites of possible focal mechanism solutions for both events. The suites of solutions for each event, which are remarkably similar, are available as an electronic supplement to this paper (© Fig. S1, see supplement); a summary focal mechanism for both events is shown in Figure 4.

DISCUSSION

Active seismicity in the area of Roosevelt Lake and the apparent swarm-like nature of the 2007 cluster could be explained by a number of causes, including reservoir induced seismicity (RIS), migration of hydrothermal fluids at depth, or brittle failure due to the release of regional tectonic stresses. Each potential explanation for the observed cluster carries significant implications for the overall geology and tectonics within the region. Here we evaluate these possible causes, considering suites of other local and regional constraints.

Previous studies have determined that RIS can extend outward from a reservoir by a factor of 3 to 4 times the reservoir width (Talwani *et al.*, 2007). At its widest point, Roosevelt Lake is 3.5 km across; a conservative estimate of the potential impact area of RIS, therefore, is ~ 10.5 km from the reservoir

Table 1
Earthquakes Recorded in the Vicinity of Theodore Roosevelt Lake

Event ID	Date (MM/DD/YYYY)	Origin Time (GMT) (HH:MM:SS)	Latitude Longitude		Depth (km)	Magnitude (M_L)	Event Family	# Arrivals Picked
			Latitude	Longitude				
B	12/11/1979	20:35:00	33.650	-111.100	0	2.5	-	-
1	06/21/2007	10:40:42	33.731	-111.137	5	1.4	1a	13
2	06/25/2007	13:04:55	33.729	-111.139	5	2.7	1b	18
3	06/25/2007	13:06:59	33.727	-111.134	7	1.3	1c	5
4	06/25/2007	13:07:08	33.725	-111.133	9	1.4	1b	17
5	06/25/2007	13:07:46	33.734	-111.140	7	1.1	1b	12
6	06/25/2007	13:51:07	33.725	-111.134	8	0.2	1a	4
7	06/25/2007	14:17:56	33.728	-111.134	9	1.2	1c	11
8	06/25/2007	14:50:43	33.730	-111.141	8	0.3	2	5
9	06/25/2007	14:52:28	33.730	-111.140	7	3.1	1	18
10	06/25/2007	14:56:27	33.729	-111.134	9	1.5	2	16
11	06/25/2007	15:06:43	33.729	-111.135	9	1.1	2	7
12	06/25/2007	16:23:07	33.730	-111.137	8	0.4	1d	6
13	06/25/2007	19:36:25	33.730	-111.137	6	1.5	1d	12
14	06/25/2007	19:57:21	33.728	-111.135	9	0.4	1c	7
15	06/25/2007	20:49:46	33.730	-111.138	8	0.5	1e	6
16	06/26/2007	08:13:56	33.732	-111.141	6	1.5	1e	16
17	06/26/2007	15:39:14	33.728	-111.141	1	0.8	2	8
18	06/27/2007	08:34:50	33.728	-111.136	8	0.1	1	7
19	06/28/2007	13:29:19	33.727	-111.134	8	0.5	1	4
20	06/28/2007	20:27:16	33.729	-111.138	8	0.3	1e	7
21	01/27/2008	01:28:39	33.640	-111.124	5	0.9	3	9
22	01/27/2008	09:42:33	33.635	-111.119	9	-	3	5
A	05/03/2008	10:29:32	33.714	-111.063	0	1.0	-	-
B	06/25/2010	10:30:34	33.610	-111.196	5	3.1	-	-
B	09/26/2010	22:20:31	33.696	-111.147	5	2.8	-	-

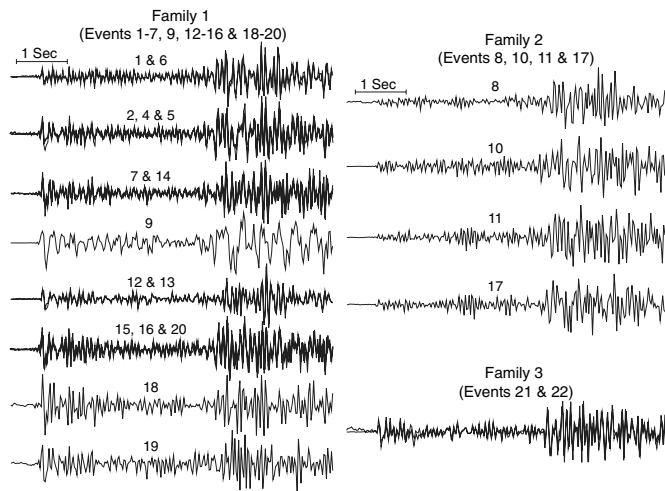
A, recorded by USArray TA (Lockridge *et al.*, 2012); B, from Arizona event catalog assembled by Lockridge *et al.* (2012).

edges. All known historical events (Table 1) in the Roosevelt Lake area, as well as the events discovered in this study, are within this distance from the edge of the reservoir, and are therefore potential candidates for RIS.

To evaluate the potential impact of the Roosevelt Lake on local seismicity, we obtained daily reservoir water levels from Salt River Project (SRP), the owner and operator of Roosevelt Dam (see Data and Resources section). Daily water levels from March 2006 through September 2010 are plotted in Figure 5, with the five known periods of seismic activity during that period also plotted for reference. In comparing each of the five most recent instances of seismic activity to reservoir water levels during the same time period, we note that (1) the June 2007 cluster occurs during a water-level drop following a year of low-water levels, (2) the 27 January 2008 events occur at the beginning of a large water-level increase, (3) the 3 May 2008 event occurs in the weeks following a water level peak, (4) the 25 June 2010 event occurs approximately 90 days following the high-water mark for the time of the study, and (5) the 26 September 2010 event occurs during a gradual decline in

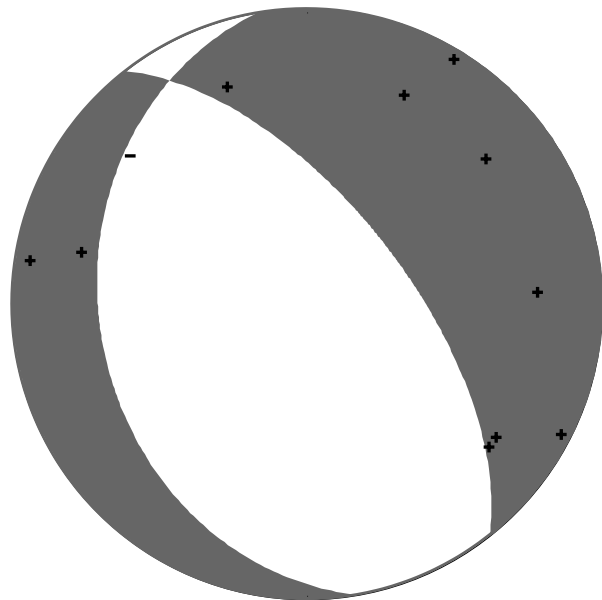
water level. From the available data, no clear temporal correlations between reservoir water levels and seismic activity are observed; however, a 90-day delay from peak seismicity for the 25 June 2010 event could be adequate to allow for pore-pressure diffusion from RIS, assuming typical permeability levels of 0.1–100 m²/s determined to be necessary for RIS (e.g., Talwani and Acree, 1985).

Known occurrences of RIS are classified as either initial or protracted seismicity. Initial RIS occurs following the initial impoundment of a reservoir or when water levels increase above a previous high-water mark. In most cases, seismicity returns to background levels after a period of months to years. Protracted RIS occurs more rarely, can continue for years or decades after initial impoundment, and is dependent on the frequency and amplitude of water-level changes (Talwani, 1997). The December 1979 earthquake is the only known historical event located in the vicinity of Roosevelt Lake that occurred prior to the deployment of the TA; therefore, we rule out the possibility of initial RIS for the events in our dataset. Further, we observe no temporal correlation between recent

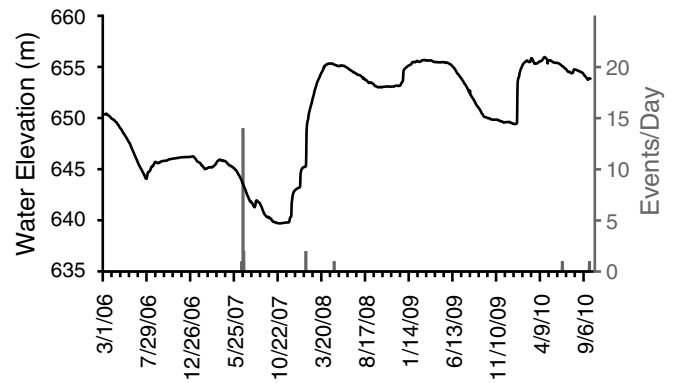


▲ **Figure 3.** Event families recorded during the Roosevelt Lake earthquake cluster. Waveforms are vertical component only from station Y17A. Family 1 includes events with impulsive P arrivals; Family 2 is characterized by weak P arrivals. Numbers above each trace correspond to the chronological order in which the event occurred.

seismicity and water level fluctuations at Roosevelt Lake (Fig. 5). These findings are consistent with Anderson *et al.* (1987), who also considered the occurrence of RIS at Roosevelt Lake to be very unlikely. However, due to the small amount of



▲ **Figure 4.** Summary focal mechanism solution (170° strike, 30° dip, -65° rake) for the two largest (M_L 3.1 and 2.7) earthquakes in the June 2007 Roosevelt Lake earthquake cluster. Arrival polarities for the largest (M_L 3.1 6/25/2007 14:52:28 GMT) earthquake in the sequence are identified as compression (+) and dilatation (-). The entire suite of viable focal mechanism solutions is available as an electronic supplement to this paper (© Fig. S1, see supplement).



▲ **Figure 5.** Comparison of reservoir water elevation above mean sea level (black, left vertical axis) and the number of earthquakes recorded per day (grey, right vertical axis). Tick marks on the horizontal axis represent 30 days of data and are labeled every 150 days. The peaks in the events per day series represent the June 2007 earthquake cluster, the two 27 January 2008 earthquakes, the 3 May 2008 event, the 25 June 2010 earthquake, and the 26 September 2010 earthquake (see Table 1; Fig. 2).

measured seismicity and the duration of our investigation, further monitoring of small-scale seismicity in the area is warranted to definitively rule out the occurrence of protracted RIS at Roosevelt Lake.

As an alternative to RIS, we consider that swarm-like clusters of seismicity often occur in response to the migration of hydrothermal fluids or magma at depth (Špičák, 2000; Rabak *et al.*, 2010; Heinicke *et al.*, 2009; Farrell *et al.*, 2009; Halloween 2009 swarm near Sunset Crater, Arizona [see Data and Resources section]). Regional heat flow in the Roosevelt Lake region is ~ 90 – 100 mW/m^2 (see Data and Resources section), suggesting that subsurface migration of hydrothermal fluids may exist. However, the most recent volcanic units within Tonto Basin were deposited from 23 to 19 Ma (Anderson *et al.*, 1987), and earthquake clusters with volcanic origins are typically swarm-like, with no clear mainshock occurring at the beginning of a sequence of increased seismicity rates. For the 2007 Roosevelt Lake cluster, the event frequency was highest immediately following the two largest (M_L 2.7 and 3.1) events and decreases with time later in the cluster, which is consistent with mainshock–aftershock sequences of tectonic origin.

Potential focal mechanism solutions for the two largest events in the 2007 cluster are consistent with northwest–southeast trending normal faults and contain a small component of strike slip motion. Since stations used, arrival polarities, and takeoff angles are similar for both of the earthquakes, families of potential focal plane solutions (© Fig. S1, see supplement) were nearly identical for both events and we summarize them together in Figure 4. A northwest–southeast normal fault plane is consistent with the overall trend of focal mechanisms from historical earthquakes located throughout the ATZ and southern CP (see Kreemer *et al.*, 2010 and references therein). Further, Pearthree *et al.* (1983) found that Quaternary faulting in central and southern Arizona typically occurs along

pre-existing structures. Mapped faults within the Roosevelt Lake area are generally northwest striking and include the southwest-dipping Armer Mountain fault and the northeast-dipping Two Bar North fault (Fig. 2; Anderson *et al.*, 1987). The existing fault orientations are consistent with both of the potential fault plane solutions represented in the focal mechanism data (Fig. 4, ⊕ Fig. S1, see supplement); therefore, the available seismic and geologic data support the hypothesis that earthquakes in the area of Roosevelt Lake are tectonic in origin.

In an effort to determine whether to expect surface rupture from the largest events in the 2007 Roosevelt Lake sequence as well as other recent ATZ events of similar magnitude, we examine the total energy release and potential fault slip range during the Roosevelt Lake cluster. We converted M_L to seismic moment (M_0) and moment magnitude (M_w) for each event using equations from Hanks and Kanamori (1979):

$$\log M_0 = 1.5M_L + 16.0$$

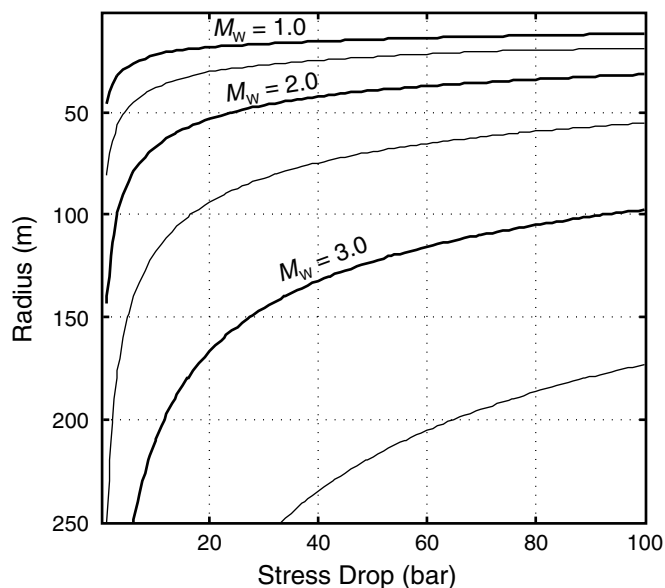
$$M_w = 2/3 \log M_0 - 10.7$$

We used the computed M_0 values to calculate a range of potential event radii (c) and stress drops ($\Delta\sigma$) for each event following Hanks (1977):

$$M_0 = 16/7 * \Delta\sigma c^3$$

From these equations, we computed that the potential radius of slip for an event of similar magnitude to the M_L 3.1 event ranges from approximately 100 to 120 m for realistic stress drop values of 60 to 100 bar (Fig. 6). We also found that a small event of M_w 1.0 would have a potential radius of slip ranging from 10 to 12 m for realistic stress drop values. These results suggest that small magnitude events and event clusters can release stress from continued B&R extension within the ATZ without generating surficial geomorphic evidence of rupture (e.g., Eagar and Fouch, 2007).

In a separate study encompassing the entire state of Arizona, Lockridge *et al.* (2012) found that 58% of events recorded by the TA were located at least 10 km from documented Quaternary faults, including most events and event clusters within the ATZ and southern B&R provinces. These small events throughout central and southern Arizona may represent either residual pulses of activity from the B&R disturbance or the development of a new, small-scale system of post-B&R extension (Menges and Pearthree 1989). Recurrence intervals for documented normal faults in the southern B&R province range from 10,000 to 100,000 years (Pearthree and Calvo, 1987; Menges and Pearthree, 1989); however, these studies are limited to large faults with surficial evidence of rupture. We suggest, therefore, that localized small-scale seismicity is a likely means by which the southern and central Arizona region releases the majority of the stress associated with continued crustal deformation. The dearth of historically recorded events within the ATZ and B&R regions of Arizona is likely due to the absence of seismic monitoring stations rather than an absence of seismic activity.



▲ **Figure 6.** Relationship between slip radius, stress drop, and magnitude for a penny-shaped crack fault model. Contour lines correspond to magnitude values as labeled. We note that for an assumed stress drop of 100 bar, the fault plane for an M_w 3.0 earthquake (similar to the largest in this study) would have a radius of ~100 m.

CONCLUSIONS

The recent deployment of the USArray TA enables the identification of seismicity centered at multiple locations surrounding Roosevelt Lake. Multiple periods of seismic activity coupled with the lack of correlation between seismicity and reservoir water levels suggests that this portion of the ATZ continues to experience active tectonic deformation due to regional stresses. Focal mechanisms for the largest two events in the area are consistent with a northwest–southeast trending normal fault, which corresponds well with locally mapped lineaments and suggests a reactivation of preexisting structures. The presence of scattered seismic activity in the area of Roosevelt Lake from 1979 to 2010 may warrant additional monitoring in order to improve the characterization of the local stress field.

DATA AND RESOURCES

USArray Array Network Facility (ANF) provided waveforms, databases, and initial event location data (<http://anf.ucsd.edu/tools/events/download.php>, last accessed May 2011) used to initiate this study. We utilized the Antelope Environmental Data Collection Software suite (<http://www.brtt.com>, last accessed May 2011) for waveform analysis and earthquake location. Current and historical earthquake data used in this study were obtained from a catalog assembled by Lockridge *et al.* (2012). Regional heat flow data used in this study are available from the SWGEONET geophysical database (Yoburn *et al.*, 2006). We obtained historical reservoir water levels for Roosevelt Lake via

personal communication with Tim Skarupa at SRP. Digital geologic maps of Arizona used in this study (Richard *et al.*, 2002) are available from http://www.azgs.az.gov/services_azgeomap.shtml (last accessed June 2011). ☒

ACKNOWLEDGMENTS

We thank Frank Vernon and the EarthScope USArray Array Network Facility for providing wave form data and preliminary event data, the EarthScope USArray Transportable Array team for the installation and maintenance of stations used in this study. We also thank Jeri Young, Phil Pearthree, David Simpson, Frank Vernon, Susan Beck, and Diana Roman for productive discussions and useful reference materials. We acknowledge helpful comments by an anonymous reviewer and SRL editor Jonathan Lees. This work was supported by the Arizona Geological Survey/Arizona Department of Emergency Management via a grant from the Federal Emergency Management Agency to JRA and MJF, and by the National Science Foundation via an EarthScope Science CAREER grant to MJF (EAR-0548288).

REFERENCES

- Anderson, L. W., L. A. Piety, and R. C. LaForge (1987). Seismotectonic investigation, Theodore Roosevelt Dam, Salt River Project Arizona, *U. S. Bureau of Reclamation Seismotectonic Rept. No. 87-5*, 46 pp.
- Bashir, L., S. S. Gao, K. H. Liu, and K. Mickus (2011). Crustal structure and evolution beneath the Colorado Plateau and the southern Basin and Range Province: Results from receiver function and gravity studies, *G-cubed* **12**, Q06008.
- Brumbaugh, D. S. (1980). Analysis of the Williams, Arizona earthquake of November 4, 1971, *Bull. Seismol. Soc. Am.* **70**, 885–891.
- Brumbaugh, D. S. (1987). A tectonic boundary for the southern Colorado plateau, *Tectonophysics* **136**, 125–136.
- Eagar, K. C., and M. J. Fouch (2007). Detection of a unique earthquake swarm in eastern Arizona, *Arizona Geol.* **37**, 1–5.
- Eberhart-Phillips, D., R. M. Richardson, M. L. Sbar, and R. B. Hermann (1981). Analysis of the 4 February 1976 Chino Valley, Arizona earthquake, *Bull. Seismol. Soc. Am.* **71**, 787–801.
- Farrell, J., S. Husen, and R. B. Smith (2009). Earthquake swarm and *b*-value characterization of the Yellowstone volcano-tectonic system, *J. Volcanol. Geoth. Res.* **188**, 260–276.
- Frassetto, A., H. Gilbert, G. Zandt, S. Beck, and M. J. Fouch (2006). Support of high elevation in the southern Basin and Range based on the composition and architecture of the crust in the Basin and Range and Colorado Plateau, *Earth Planet. Sci. Lett.* **249**, 62–73.
- Gilbert, H. (2012). Crustal structure and signatures of recent tectonism as influenced by ancient terranes in the western United States, *Geosphere* **8**, 141–157.
- Gupta, H. K. (2002). A review of recent studies of triggered earthquakes by artificial water reservoirs with special emphasis on earthquakes in Koyana, India, *Earth Sci. Rev.* **58**, 279–310.
- Hanks, T. C. (1977). Earthquake stress drops, ambient tectonic stresses and stresses that drive plate motions, *Pure Appl. Geophys.* **115**, 441–458.
- Hanks, T. C., and H. Kanamori (1979). A moment-magnitude scale, *J. Geophys. Res.* **84**, 2348–2350.
- Havskov, J., and L. Ottemöller (1999). SeisAn earthquake analysis software, *Seismol. Res. Lett.* **70**, 532–534.
- Heinicke, J., T. Fischer, R. Gaupp, J. Götze, U. Koch, H. Konietzky, and K.-P. Stanek (2009). Hydrothermal alteration as a trigger mechanism for earthquake swarms: The Vogtland/NW Bohemia region as a case study, *Geophys. J. Internat.* **178**, 1–13.
- Hendricks, J. D., and J. B. Plescia (1991). A review of the regional geophysics of the Arizona transition zone, *J. Geophys. Res.* **96**, 12,351–12,373.
- Kreemer, C., G. Blewitt, and W. C. Hammond (2010). Evidence for an active shear zone in southern Nevada linking the Wasatch fault to the Eastern California shear zone, *Geology* **38**, 475–478.
- Lockridge, J. S., M. J. Fouch, and J. R. Arrowsmith (2012). Seismicity within Arizona during the Deployment of the EarthScope USArray Transportable Array, *Bull. Seismol. Soc. Am.* **102**, 4, 1850–1863, doi: [10.1785/0120110297](https://doi.org/10.1785/0120110297).
- Ma, S., and D. W. Eaton (2011). Combining double-difference relocation with regional depth-phase modeling to improve hypocentre accuracy, *Geophys. J. Int.* **185**, 871–889.
- Ma, S., and D. W. Eaton (2009). Anatomy of a small earthquake swarm in southern Ontario, Canada, *Seismol. Res. Lett.* **80**, 214–223.
- Ma, S., D. W. Eaton, and J. Adams (2008). Intraplate seismicity of a recently deglaciated shield terrane: A case study from Northern Ontario, Canada, *Bull. Seismol. Soc. Am.* **98**, 2828–2848.
- McQuarrie, N., and B. P. Wernicke (2005). An animated tectonic reconstruction of southwestern North America since 36 Ma, *Geosphere* **1**, 147–172.
- Menges, C. M., and P. A. Pearthree (1983). Map of neotectonic deformation in Arizona, *Arizona Bureau of Geology and Mineral Technology Open-File Rept. 83-22*, scale 1:500,000.
- Menges, C. M., and P. A. Pearthree (1989). Late Cenozoic tectonism in Arizona and its impact on regional landscape evolution, in *Geologic Evolution of Arizona*, Arizona Geological Society, Digest No. 17, 649–680.
- Pavlis, G. L., F. Vernon, D. Harvey, and D. Quinlan (2004). The generalized earthquake-location (GENLOC) package: An earthquake-location library, *Comput. Geosci.* **30**, 1079–1091.
- Pearthree, P. A., and S. S. Calvo (1987). The Santa Rita fault zone: Evidence for large magnitude earthquakes with very long recurrence intervals, Basin and Range province of southeastern Arizona, *Bull. Seismol. Soc. Am.* **77**, 97–116.
- Pearthree, P. A., and R. B. Scarborough (1984). Reconnaissance analysis of possible Quaternary faulting in central Arizona, *Arizona Bureau of Geology and Mineral Technology Open-File Rept. 85-4*, scale 1:250,000, 75 pp.
- Pearthree, P. A., C. M. Menges, and L. Mayer (1983). Distribution, recurrence, and possible tectonic implications of late Quaternary faulting in Arizona, *Arizona Bureau of Geology and Mineral Technology Open-File Rept. 83-20*, 36 pp.
- Peirce, H. W. (1984). The Mogollon escarpment, *Arizona Bureau of Geology and Mineral Technology Fieldnotes*, **4**, 8–11.
- Rabak, I., C. Langston, P. Bodin, S. Horton, M. Withers, and C. Powell (2010). The Enola, Arkansas, intraplate swarm of 2001, *Seismol. Res. Lett.* **81**, 549–559.
- Richard, S. M., S. J. Reynolds, J. E. Spencer, and P. A. Pearthree (2002). Geologic Map of Arizona, a representation of Arizona Geological Survey Map 35, v.1.0, *Arizona Geological Survey: Digital Geological Map DGM-17*.
- Richter, C. F. (1935). An instrumental earthquake magnitude scale, *Bull. Seismol. Soc. Am.* **25**, 1–32.
- Simpson, D. W., W. S. Leith, and C. H. Scholz (1986). Two types of reservoir-induced seismicity, *Bull. Seismol. Soc. Am.* **78**, 2025–2040.
- Sinno, Y. A., G. R. Keller, and M. L. Sbar (1981). A crustal seismic refraction study in west-central Arizona, *J. Geophys. Res.* **86**, 5023–5038.
- Snoke, J. A., J. W. Munsey, A. G. Teague, and G. A. Bollinger (1984). A program for focal mechanism determination by combined use of polarity and *Sv-P* amplitude ratio data, *Earthquake Notes* **55**, 15–20.

- Špičák, A. (2000). Earthquake swarms and accompanying phenomena in intraplate regions: a review, *Studia Geophysica et Geodaetica* **44**, 89–106.
- Talwani, P. (1997). On the nature of reservoir induced seismicity, *Pure App. Geophys.* **150**, 473–492.
- Talwani, P., and S. Acree (1985). Pore pressure diffusion and the mechanism of reservoir-induced seismicity, *Pure App. Geophys.* **122**, 947–965.
- Talwani, P., L. Chen, and K. Gahalaut (2007). Seismogenic permeability, k_s , *J. Geophys. Res.* **112**, 18 pp., B07309, doi: [10.1029/2006JB004665](https://doi.org/10.1029/2006JB004665).
- Thompson, G. A., and M. L. Zoback (1979). Regional geophysics of the Colorado Plateau, *Tectonophysics* **61**, 149–181.
- Uski, M., T. Tiira, A. Korja, and S. Elo (2006). The 2003 earthquake swarm in Anjalankoski, southeastern Finland, *Tectonophysics* **422**, 55–69.
- Yoburn, J. B., M. J. Fouch, J. R. Arrowsmith, and G. R. Keller (2006). A new GIS-driven geophysical database for the southwestern United States, in *Geoinformatics: Data to Knowledge: Geological Society of America Special Paper 397*, A. K. Sinha (Editor), 249–267.
- Zoback, M., R. E. Anderson, and G. A. Thompson (1981). Cainozoic evolution of the state of stress and style of tectonism of the Basin and Range province of the western United States, *Phil. Trans. Roy. Soc. Lond. A* **300**, 407–434.

Jeffrey S. Lockridge
 Matthew J. Fouch¹
 J Ramón Arrowsmith
 School of Earth and Space Exploration
 Arizona State University
 PO Box 871404
 Tempe, Arizona 85287-1404 U.S.A.
 Lockridge@asu.edu

Lepolt Linkimer²
 Department of Geosciences
 University of Arizona
 Gould-Simpson Building 77
 Tucson, Arizona 85721 U.S.A.

¹ Now at Department of Terrestrial Magnetism, Carnegie Institution of Washington, 5241 Broad Branch Road, NW, Washington, D.C. 20015 U.S.A.

² Now at Escuela Centroamericana de Geología, Apartado 214-2060, Universidad de Costa Rica, San José, Costa Rica.